

Phenotype Screening of an Azole-bisindole Chemical Library Identifies URB1483 as a New Antileishmanial Agent Devoid of Toxicity on Human Cells

Aurora Diotallevi, Laura Scalvini, Gloria Buffi, Yolanda Pérez-Pertejo, Mauro De Santi, Michele Verboni, Gianfranco Favi, Mauro Magnani, Alessio Lodola, Simone Lucarini,* and Luca Galluzzi



Cite This: *ACS Omega* 2021, 6, 35699–35710



Read Online

ACCESS |



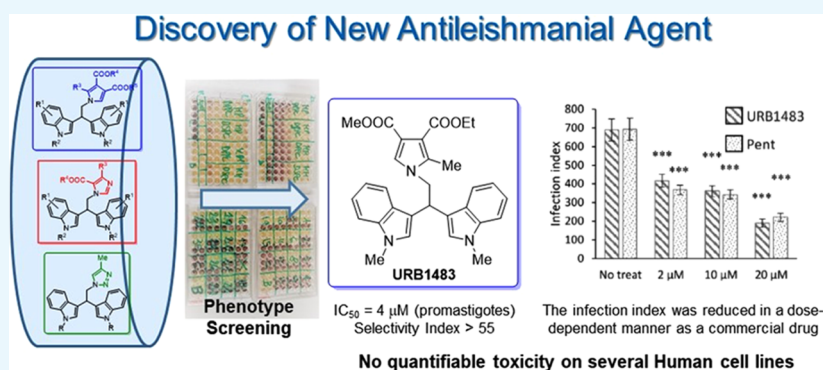
Metrics & More



Article Recommendations



Supporting Information



ABSTRACT: We report the evaluation of a small library of azole-bisindoles for their antileishmanial potential, in terms of efficacy on *Leishmania infantum* promastigotes and intracellular amastigotes. Nine compounds showed good activity on *L. infantum* MHOM/TN/80/IPT1 promastigotes with IC₅₀ values ranging from 4 to 10 μM. These active compounds were also tested on human (THP-1, HEPG2, HaCaT, and human primary fibroblasts) and canine (DH82) cell lines. **URB1483** was selected as the best compound, with no quantifiable cytotoxicity in mammalian cells, to test the efficacy on intracellular amastigotes. **URB1483** significantly reduced the infection index of both human and canine macrophages with an effect comparable to the clinically used drug pentamidine. **URB1483** emerges as a new anti-infective agent with remarkable antileishmanial activity and no cytotoxic effects on human and canine cells.

INTRODUCTION

Leishmaniasis is a neglected disease caused by protozoan parasites transmitted by phlebotomine sandflies. More than 20 different *Leishmania* species all over the world cause a variety of clinical conditions broadly grouped in cutaneous (CL), mucosal (ML), and visceral leishmaniasis (VL).¹ The latter, being fatal if untreated, causes 20 000–40 000 deaths across the globe each year.^{2,3} More than a million new cases are reported per year and 350 million people are at risk of contracting the infection.¹ Italy is an endemic country, with an increase in cases in the last two decades due to said disease spreading within traditionally endemic regions and to the appearance of autochthonous cases in previously nonendemic areas such as northern continental Italy.^{2,4} The most widespread form of leishmaniasis endemic in southern Europe is zoonotic VL, involving humans and domestic dogs (which may serve as the main reservoir), sometimes associated with a few cases of CL. Both diseases are caused by *L. infantum*.⁴

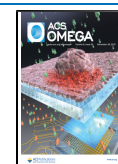
Although in recent years three vaccine candidates have undergone clinical trials, and half a dozen more are in the

pipeline, no efficacious vaccine against leishmaniasis is now available on the market.⁵ Moreover, all currently available drugs are inadequate¹ (Figure 1). Pentavalent antimonials (one example is meglumine antimoniate, Figure 1), the first-line treatment, could not be efficacious due to widespread resistance to the drug. A few treatments against leishmaniasis have been introduced during the last decade, each of them having serious limitations. Amphotericin B, one of the most used second-line drugs, is effective against antimonial-resistant *Leishmania* strains, but it can induce acute and chronic toxicity. The Amphotericin B liposomal formulation (AmBisome) ameliorates the toxicity profile; yet its high formulation cost has limited its use.⁶ Miltefosine is a highly potent oral drug

Received: October 8, 2021

Accepted: November 29, 2021

Published: December 15, 2021



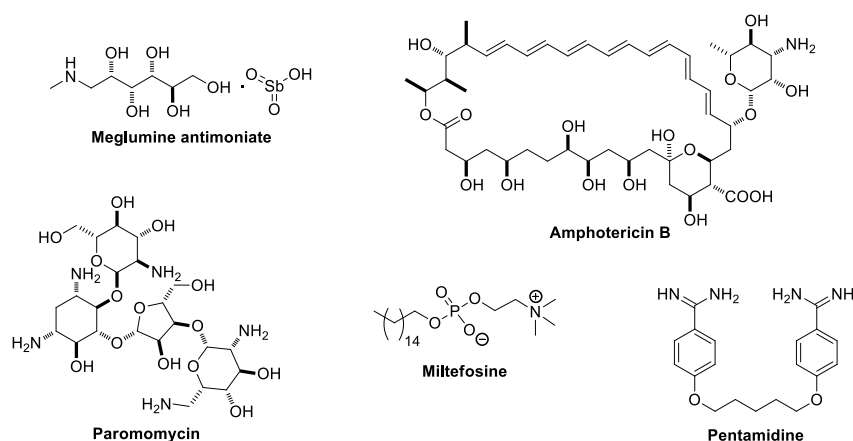


Figure 1. Main commercial drugs against Leishmaniasis.

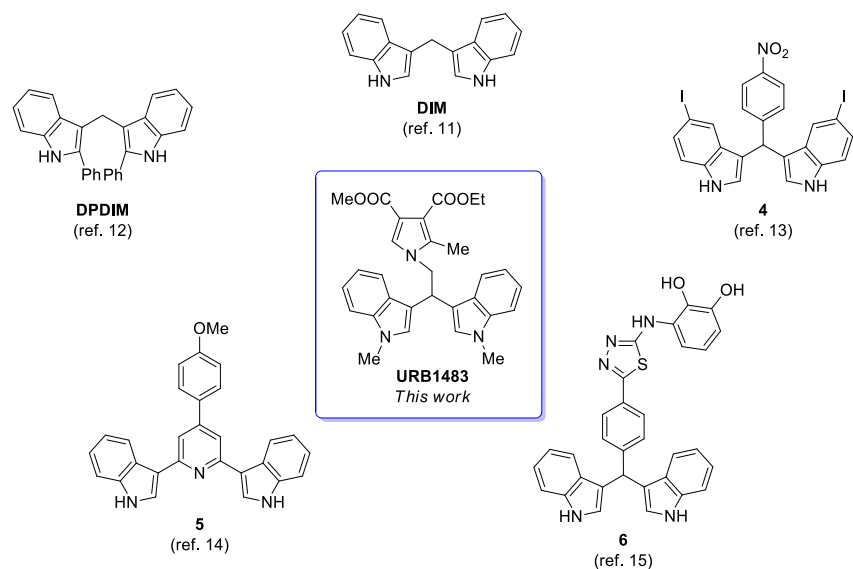


Figure 2. Potential antileishmanial agents sharing bis(indolyl) fragment.

against VL and CL; however, its use is limited due to high cost, teratogenicity, and long treatment. Paromomycin is the cheapest treatment, but its use has been associated with severe toxicity. Moreover, this drug requires parenteral administration, needs long treatment, and shows region-dependent efficacy. On the other hand, pentamidine is used in combination therapies at low dosages but shows several shortcomings (renal toxicity, myocarditis, diabetes mellitus, hypoglycemia, hypotension, and fever).¹

Due to the serious drawbacks of the available therapeutic options, shorter courses and inexpensive drugs, less toxic and more efficacious across all endemic regions, are urgently needed. Many research groups around the world have developed several new scaffolds as potential drugs against leishmaniasis.^{1,7–10} Among them, a few bisindoles were reported (Figure 2).

The seminal work of Roy and his collaborators reported that 3,3'-diindolylmethane (DIM, Figure 2) is an effective inhibitor of *L. donovani* topoisomerase IB.¹¹ More specifically, the prototypical member of the class, DIM, was reported to act as poison for topoisomerase IB, i.e., similar to the well-known drug camptothecin (CPT), it stabilizes the topoisomerase–DNA cleavage complex, thus blocking the relaxation process.^{11,12} In subsequent work, the same authors reported

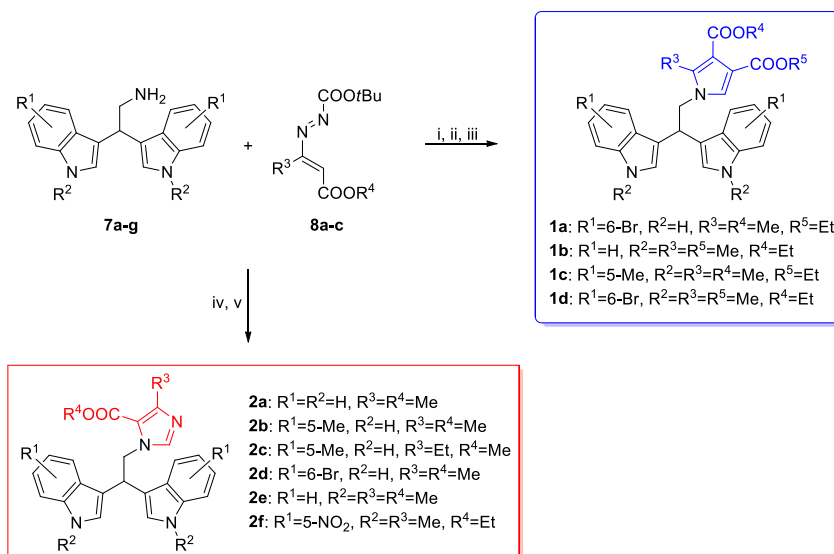
three new DIM derivatives that were active against a DIM-resistant strain of *L. donovani*. In Figure 2, 2,2'-diphenyl-3,3'-diindolylmethane (DPDIM) is shown as the most promising example of the reported DIMs.

Moreover, the methylene linker of DIM represents an ideal point of chemical diversification that can be exploited to generate a library of compounds useful for phenotype screening. This strategy has been shown to be affordable and practical also by other authors^{13–15} who used a six-membered aromatic ring as an additional side arm (i.e., compounds 4 and 6) or a spacer connecting the two indolyl moieties (compound 5) in different sets of DIM analogues obtaining new potent antileishmanial agents.

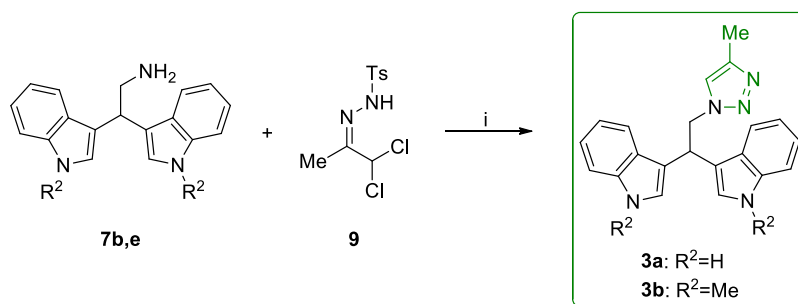
In detail, Bharate and co-workers reported in 2013 a new aryl-DIM potent class of antileishmanial agents. Among them, compound 4 (Figure 2) was the most effective against *L. donovani* promastigotes and amastigotes, showing IC₅₀ values lower than 10 μM.¹³ However, they did not propose a biological target of the new aryl-DIMs.

Bis(indolyl)-pyridine 5 (Figure 2) is the most interesting compound reported by Kalam Khan et al. against *Leishmania* parasites,¹⁴ but it is less potent than previously described DIMs and no information about its mechanism of action is available. Very recently, the group of Taha has reported several phenyl-

Scheme 1. Reagents and Conditions: (i) Methyl or Ethyl (R^5) Propiolate, DCM, at Room Temperature (rt), Overnight; (ii) 1,2-Diaza-1,3-diene 8, Toluene, Reflux, 2 h; (iii) TFA, Reflux, 2–4 h; (iv) 1,2-Diaza-1,3-diene 8, ACN, rt, 1 h; (v) Paraformaldehyde, Reflux, 4 h



Scheme 2. Reagents and Conditions: (i) DIPEA, Ethanol, 9 in Acetonitrile, 0 °C to rt, 2 h



aminothiazole-DIM derivatives as potent antileishmanial agents.¹⁵ In particular, compound **6** (Figure 2) has shown an outstanding effect on the protozoa with a submicromolar IC_{50} value. The authors claimed that this new class of compounds may inhibit the pteridine reductase. Yet, no inhibition studies on the isolate enzyme were reported.

As part of our ongoing investigations on the biological activities and applications of bisindole derivatives^{16–20} and leishmaniasis,^{21–24} in the present study, a focused library of selected published azole-bisindole derivatives **1–3** (Schemes 1 and 2)^{20,25} sharing the bis(indolyl) motif with the above-mentioned antileishmanial agents and presenting an additional azole side arm was screened against several human and canine *L. infantum* promastigote strains. The most active compounds ($IC_{50} < 20 \mu\text{M}$) were then tested on human and canine macrophages, as well as other human cell lines to check for their potential toxicity. Pyrrole-bisindole **1b**, named **URB1483**, was found to be the most specific compound against parasites and was tested for its efficacy on *L. infantum*-infected human and canine macrophage-like cell lines.

RESULTS

Chemistry. Pyrrole-bisindoles **1a–d** and imidazole-bisindoles **2a–f** were synthesized according to previously reported methods¹⁹ starting from the opportune bisindoles **7a–g** and 1,2-diaza-1,3-diene **8a–c**^{16,20,25} (Scheme 1).

The treatment of bisindole **7** with the opportune propiolate in dichloromethane (DCM) followed by the addition of 1,2-diaza-1,3-diene **8** in toluene and in the presence of trifluoroacetic acid (TFA) at reflux furnished the corresponding pyrrole-indole **1**. The mechanism of this sequential three-component reaction involves the preliminary formation of enamine intermediate, subsequent Michael addition to azoene system, and final intramolecular heterocyclization with loss of the carbazate residue.

On the other hand, the indole-imidazole scaffold **2** was synthesized by a conjugate addition of bisindole **7** to **8** in acetonitrile (ACN) at room temperature (rt), followed by the condensation with the paraformaldehyde at reflux. For this three-component reaction, a thermal-assisted 1,5-electrocyclization of 1,2-diaza-1,3-diene-derived azavinyl azomethine ylides appears to be operative.²⁰

Triazole-bisindoles **3** were instead synthesized in a single step (Sakai's protocol) from α,α -dichlorotolylhydrazide **9** and bisindole **7**,^{16,20} respectively, in the presence of *N,N*-diisopropylethylamine (DIPEA) as a base in an ethanol/acetonitrile mixture (Scheme 2).²⁰

Effect of Bisindoles on *L. infantum* Promastigote Viability. The *in vitro* antileishmanial activity evaluation of bisindole derivatives was carried out by treating *L. infantum* MHOM/TN/80/IPT1 promastigotes for 72 h with scalar dilution 1:2 or 2:3 (from 20 to 0.31 μM) of each molecule. As

Table 1. Potency of Azole-bisindole Derivatives on *L. infantum* Promastigote Strains^a

compound	<i>L. infantum</i>			
	MHOM/TN/80/IPT1 IC ₅₀ (μM) (95% CI)	<i>L. infantum</i> canine clinical isolate 1 IC ₅₀ (μM) (95% CI)	<i>L. infantum</i> canine clinical isolate 2 IC ₅₀ (μM) (95% CI)	<i>L. infantum</i> human clinical isolate IC ₅₀ (μM) (95% CI)
1a	6.6 (6.1–7.2)	7.0 (6.5–7.5)	5.7 (5.3–6.1)	6.4 (5.4–7.5)
1b (URB1483)	3.7 (3.2–4.2)	4.1 (3.8–4.5)	3.7 (3.5–3.9)	7.2 (5.8–8.9)
1c	>20 (43%) ^{bc}	n.t. ^c	n.t. ^c	n.t. ^c
1d	>20 (11%) ^b	n.t. ^c	n.t. ^c	n.t. ^c
2a	10 (9.2–11)	6.8 (6.2–7.5)	4.8 (4.6–5.0)	8.1 (7.2–9.1)
2b	7.7 (7.0–8.4)	6.4 (6.0–6.8)	5.0 (4.7–5.3)	6.1 (5.3–7.0)
2c	10 (9.4–11)	8.7 (7.9–9.6)	6.5 (6.2–6.9)	8.6 (7.8–9.4)
2d	8.5 (7.8–9.2)	9.7 (9.2–10.1)	7.0 (6.5–7.6)	7.5 (6.8–8.3)
2e	4.9 (4.3–5.6)	4.8 (4.5–5.1)	3.6 (3.3–3.8)	5.5 (5.0–6.0)
2f	4.9 (4.4–5.4)	6.8 (6.2–7.4)	5.6 (5.3–6.0)	5.3 (4.9–5.7)
3a	>20 (22%) ^b	n.t. ^c	n.t. ^c	n.t. ^c
3b	8.1 (7.2–9.2)	5.7 (5.3–6.1)	5.3 (5.1–5.5)	7.4 (6.6–8.3)
DIM	>20 (10%) ^b	>20 (6%) ^b	>20 (12%) ^b	>20 (22%) ^b
Pent	2.6 (2.1–3.2)	1.7 (1.6–1.9)	1.4 (1.3–1.5)	1.5 (1.4–1.6)
Amph B	0.064 (0.054–0.075)	0.12 (0.12–0.13)	0.11 (0.11–0.12)	0.084 (0.075–0.092)
Milt	2.9 (2.5–3.3)	6.6 (6.0–7.2)	6.1 (5.6–6.5)	1.2 (1.0–1.5)

^aIC₅₀ values for all of the strains are reported as mean and 95% confidence interval, from at least three independent experiments. Each experimental condition was conducted at least in duplicate. ^bPercentage of inhibition at 20 μM. ^cNot tested; **Pent**: Pentamidine; **Amph B**: nonliposomal amphotericin B; **Milt**: miltefosine.

Table 2. CC₅₀ Values of Azole-bisindole Derivatives on THP-1 and DH82 Cells

compound	THP-1		DH82	
	CC ₅₀ (μM) (95% CI)	selectivity index (CC ₅₀ /IC ₅₀ ^a)	CC ₅₀ (μM) (95% CI)	selectivity index (CC ₅₀ /IC ₅₀ ^a)
1a	124 (91–193)	18.8	11.1 (8.1–14.0)	1.7
1b (URB1483)	>200 (2%) ^b	>55	>200 (15%) ^b	>55
2a	37.9 (25.2–58.6)	3.8	35.3 (29.3–42.2)	3.5
2b	26.9 (16.7–36.9)	3.5	24.8 (21.0–29.0)	3.2
2c	38.6 (26.4–59.1)	3.8	23.5 (20.0–28.9)	2.3
2d	15.4 (12.8–19.0)	1.8	18.9 (15.4–24.0)	2.2
2e	55.4 (24.6–79.6)	11.3	24.3 (20.7–29.3)	5.0
2f	35.1 (21.5–49.9)	7.2	>200 (43%) ^b	>41
3b	>200 (33%) ^b	>25	31.9 (22.6–45.5)	3.9
Pent	103 (73–179)	40.3	10.6 (7.9–12.9)	4.1
Amph B	2.8 (1.5–3.8)	45.8	>200 (42%) ^b	>3333
Milt	27.8 (22.5–35.5)	9.8	95.9 (86.2–109)	33.6

^aSelectivity index calculated considering IC₅₀ on *L. infantum* MHOM/TN/80/IPT1. ^bPercentage of inhibition at 200 μM; **Pent**: Pentamidine; **Amph B**: nonliposomal amphotericin B. **Milt**: miltefosine.

positive controls, *Leishmania* parasites were also treated with pentamidine, nonliposomal amphotericin B, and miltefosine. The compounds **1a**, **1b**, **2a–f**, and **3b** showed IC₅₀ values between 3.7 and 10 μM. Compounds **1c**, **1d**, **3a**, and **DIM** showed IC₅₀ > 20 μM and were not taken into consideration for subsequent experiments (Table 1). Next, the activity of bisindoles was evaluated on three *L. infantum* clinical isolates (two canines and one human), confirming the activity of all tested compounds (Table 1 and Supporting Information).

Cytotoxic Effect of Bisindoles in Human and Canine Cell Lines. The cytotoxicity of the most active compounds **1a**, **1b** (URB1483), **2a–f**, and **3b** was evaluated in THP-1, DH82, HEPG2, HaCaT, and human primary fibroblasts (HPF) cells, in terms of concentrations of drug required to reduce cell viability by 50% (CC₅₀). First, to test the viability of THP-1 and DH82 cells following bisindoles treatment, the cells were treated for 72 h with each compound at five different concentrations (2, 10, 20, 80, and 200 μM). Notably, URB1483 did not show quantifiable toxicity in both cell

lines. The other compounds showed a cytotoxicity >20 μM in both cell lines, with the exception of compounds **2d** (15.4 and 18.9 μM in THP-1 and DH82 cells, respectively) and **1a** (11.1 μM in DH82 cells) (Table 2 and Supporting Information).

Next, CC₅₀ was evaluated in DH82, HEPG2, and HaCaT cell lines and HPF cells after 24 h treatment with serially diluted bisindole compounds (2, 10, 20 μM). In this case, incubations were carried out for 24 h to evaluate the cytotoxicity in actively dividing cells. In these experiments, all treatments with bisindole derivatives compounds did not show cytotoxic effects at the highest dose used (20 μM), and therefore, it was not possible to calculate the CC₅₀ values. Interestingly, in these cell lines, only the reference compound nonliposomal amphotericin B showed cytotoxicity after 24 h treatment between 4.6 and 17.3 μM (Table S1, Supporting Information).

Efficacy of Compound URB1483 on *L. infantum* Intracellular Amastigotes. Based on the analysis of the IC₅₀ and CC₅₀ obtained on *L. infantum* promastigotes and

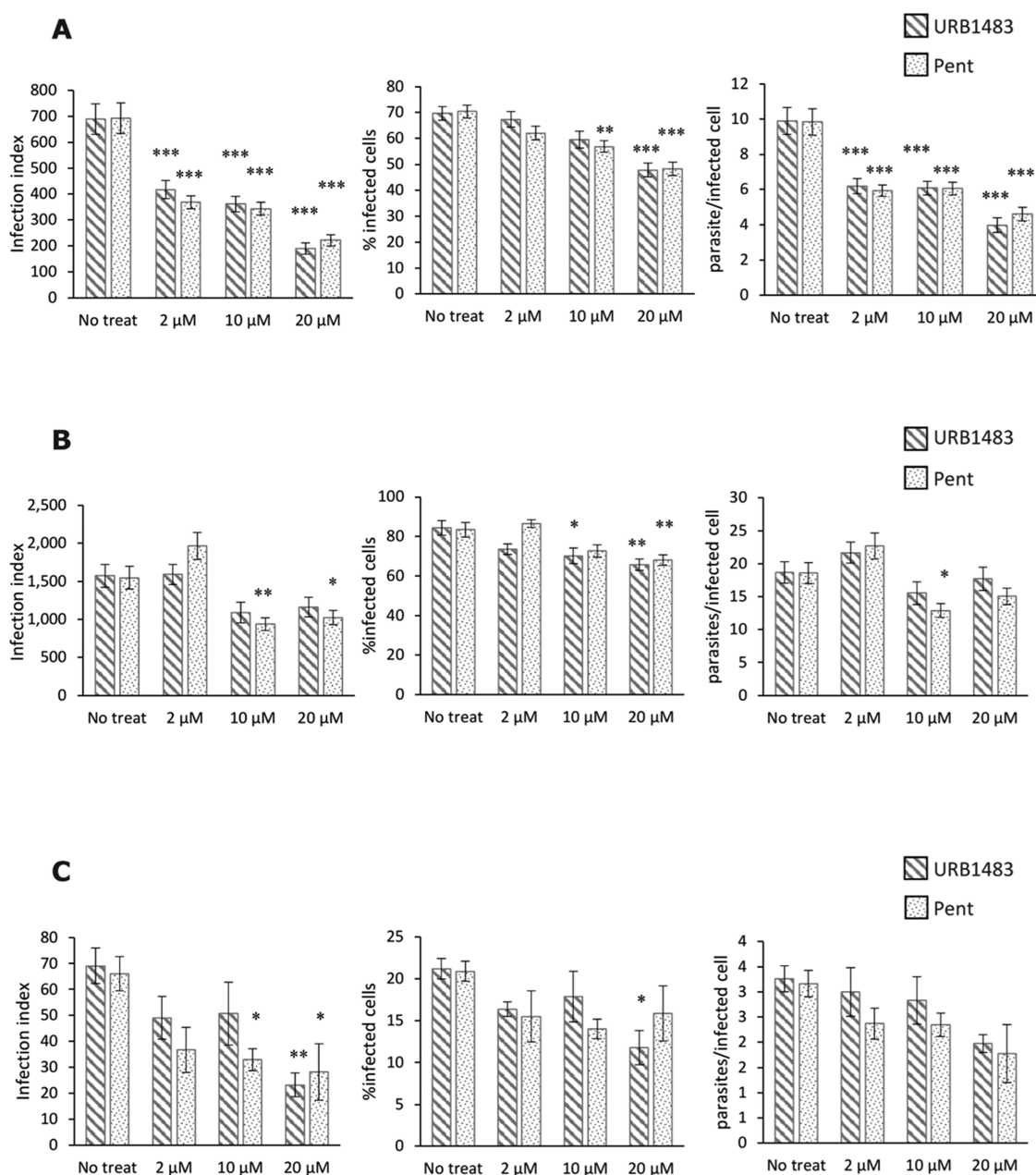


Figure 3. Effect of URB1483 and Pent on intracellular *L. infantum* amastigotes. (A) THP-1 cells infected with *L. infantum* MHOM/TN/80/IPT1; (B) THP-1 cells infected with *L. infantum* human clinical isolate; (C) DH82 cells infected with *L. infantum* MHOM/TN/80/IPT1. In all cases, cells were infected for 24 h at 37 °C; the drugs were added, and the infection index was calculated after 72 h of treatment. Data are expressed as mean \pm SEM of three independent experiments. Each experimental condition was conducted at least in duplicate. * $p < 0.05$, ** $p < 0.01$, *** $p < 0.001$.

THP-1 or DH82 cells, respectively, URB1483 was found to be the most effective and yet selective compound against the parasites and, therefore, it was selected for further experiments.

The infection of human monocytic THP-1 cell line was conducted with *L. infantum* MHOM/TN/80/IPT1 as described in the Materials and Methods section. Infected macrophages were treated with compound URB1483 or pentamidine (used as the positive control) for 72 h. The infection index was significantly reduced following the treatment with URB1483, in a dose-dependent manner (one-way ANOVA $p < 0.001$) (Figure 3a), evocative of specific mechanism of action.

Interestingly, the percentage of infected cells and the average number of amastigotes per infected cell decrease in a dose-dependent manner, in both URB1483 and pentamidine treatments. The THP-1 cells were also infected with the *L. infantum* human clinical isolate. In this case, the parasite resulted to be less susceptible to both URB1483 and Pent, compared to the reference strain MHOM/TN/80/IPT1 (Figure 3b).

The same infection and treatment protocols were also performed with the DH82 cell line. In DH82 cells infected with MHOM/TN/80/IPT1 strain, the infection index decreased significantly at the higher dose (20 μ M) in both URB1483 ($p < 0.01$) and pentamidine ($p < 0.05$) treated cells

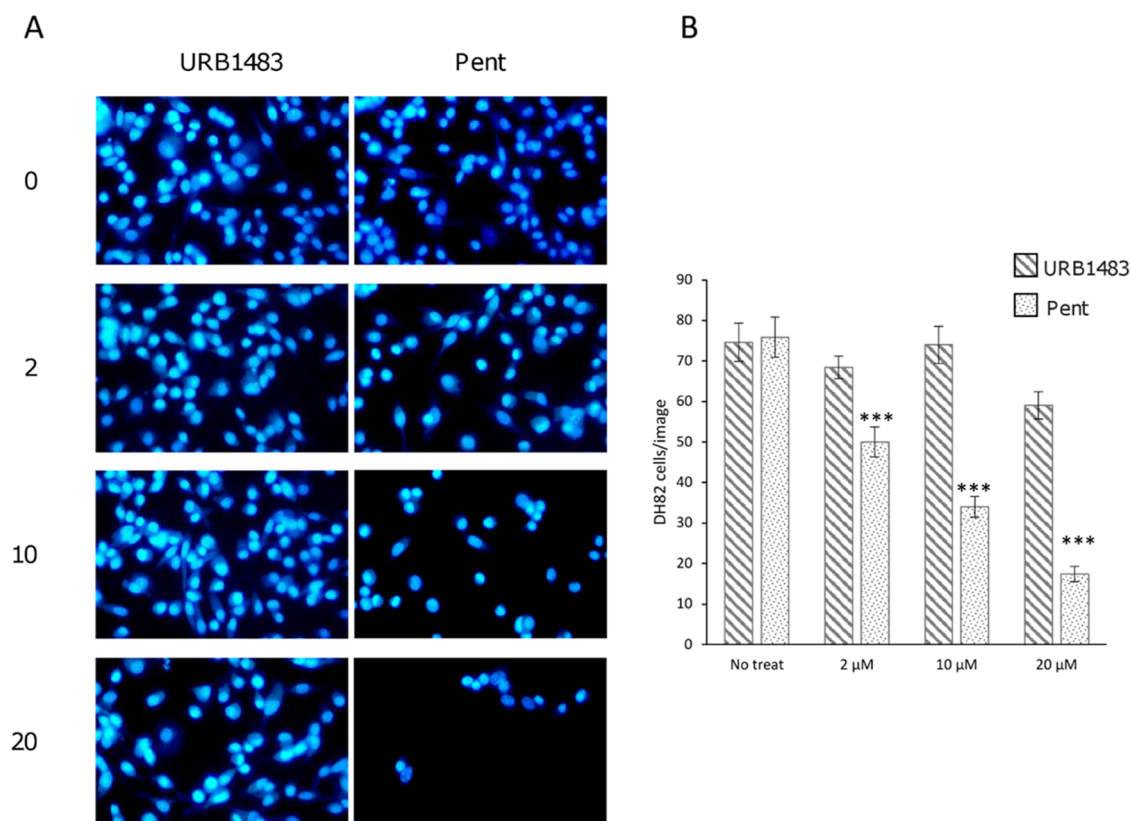


Figure 4. Cytotoxic effect of treatment with pentamidine (Pent), in contrast to URB1483, on DH82 cells after 72 h treatment. (A) Uninfected DH82 cells were treated with URB1483 or Pent for 72 h at concentrations of 0, 2, 10, and 20 μM and stained with Hoechst dye for fluorescence microscope observation. (B) Effect of treatment was monitored by calculating the number of cells, considering at least five images per treatment condition. Data are mean \pm SEM; *** $p < 0.001$.

(Figure 3c). It is noteworthy that Pent had a cytotoxic effect on DH82 cells after 72 h treatment (Table 2) (not observed after 24 h treatment), in contrast to URB1483, which did not significantly affect the cell viability (Figure 4b).

Two-way ANOVA followed by Bonferroni post hoc test did not show significant differences in infection indexes between treatments with compound URB1483 and pentamidine in all experiments (see Supporting Information Table S2), accounting for similar effects of the two molecules.

***L. donovani* Topoisomerase IB as Potential Target.**

Prompted by the encouraging results obtained on both *L. infantum* promastigote and *L. infantum* intracellular amastigotes, we searched for molecular target responsible for the antileishmanial activity displayed by compound URB1483. Literature data point to topoisomerase IB as the most likely target for bisindole compounds.^{11,12} The antileishmanial activity displayed by the bis-indolyl derivative DIM has been linked to the ability of this compound to block DNA relaxation with a mechanism similar to that of topotecan,²⁶ i.e., stabilizing the formation of a ternary complex composed of the inhibitor itself, the leishmanial enzyme topoisomerase IB, and double-strand DNA. We thus performed molecular modeling investigations assuming that URB1483 could interact with the topoisomerase IB–DNA complex by targeting the same binding site recognized by topotecan. First, a three-dimensional model of *L. donovani* topoisomerase I bound to DNA–topotecan complex was built using available structural information in the PDB, i.e., the human form of topoisomerase I bound to DNA and topotecan (PDB ID 1K4T), and the *L. donovani* form of topoisomerase I bound to nicked DNA (PDB

ID 2BS9), by following the computational protocol reported by Roy et al. (see the Materials and Methods section for details).¹² This strategy appeared reasonable as the comparison between these two topoisomerase structures reveals that, despite a diverse architecture (monomeric the human, dimeric the *L. donovani* isoform), all of the amino acid residues that line the topotecan-binding pocket are entirely conserved between the two species.²⁷

The resulting model of *L. donovani* topoisomerase IB bound to topotecan was employed to identify the binding mode for URB1483 that could account for its specific mechanism of action. Docking simulations point to a pose for URB1483 to some extent resembling the one experimentally observed for topotecan (Figure 5), with one indolyl fragment well superposed on the A-ring of topotecan and one terminal carboxylic acid ethyl ester installed on the pyrrole nucleus occupying nearly the same space of the lactone E-ring of topotecan. The second indolyl fragment of URB1483 protruded in a broad cavity of topoisomerase IB, normally occupied by solvent bulk. This additional cavity is targeted by other classes of topoisomerase poisons such as indolocarbazole and indenoisoquinoline derivatives,²⁸ which place a bulky group in this region (Figure S29, Supporting Information).

Prompted by these computational results, the inhibitory activity of URB1483 was assessed on *L. donovani* topoisomerase IB by means of a plasmid relaxation assay (Figure S30, Supporting Information). This assay detects the different electrophoretic mobility of the DNA supercoiled plasmid converted, by the enzyme, to its relaxed forms, in the presence of increasing concentrations of the compound. Gathered data

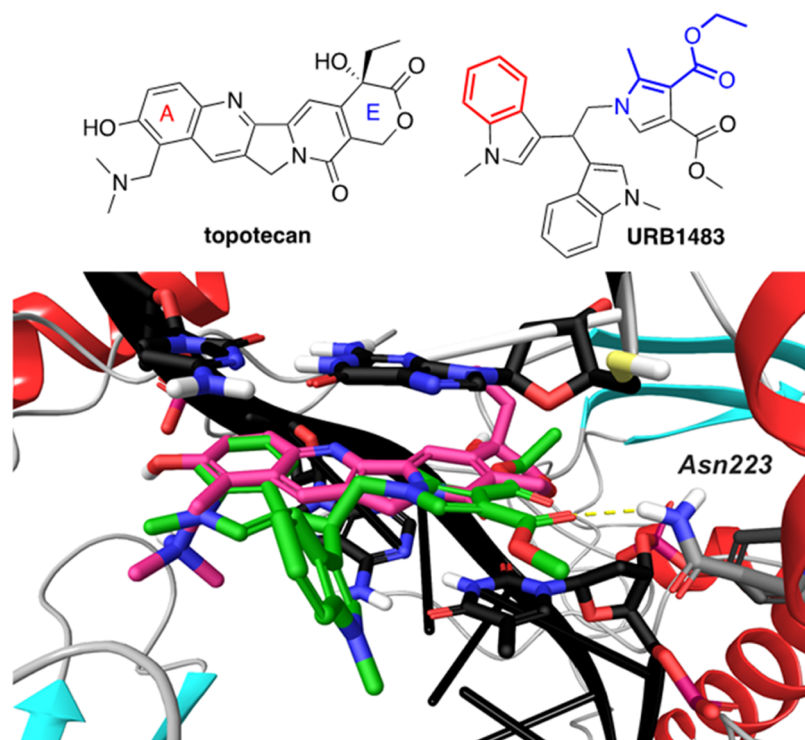


Figure 5. Molecular model of **URB1483** (green carbons) docked in the CPT binding site present in the topoisomerase IB–DNA complex (dark gray carbon atoms). The structure of topotecan (pink carbon atoms) is also displayed for comparison. The secondary structure of topoisomerase IB is represented by red (α -helices) or cyan (β -strands) cartoons, while black cartoons represent the secondary structure of the DNA (namely, 22-base pair duplex oligonucleotide).

indicate that **URB1483** does not inhibit DNA relaxation at all of the tested concentrations (up to 50 μ M).

Therefore, further investigations, not necessarily based on the structural similarity between **DIM** and **URB1483**, to identify a molecular target accounting for the anti-*Leishmania* activity of pyrrole-bisindole derivatives will be needed.

Stability Studies of URB1483. Chemical stability data were measured by LC/MS approaches for **URB1483** to preliminarily assess its *in vitro* PK profile. Gratifyingly, our analyses revealed that **URB1483** exhibited favorable chemical stability both in 0.90% w/v of NaCl water solution and in cellular medium. Under both conditions, the chemical stability was almost quantitative with more than 90% of **URB1483** remaining unaltered after 72 h.

DISCUSSION

Leishmaniasis is one of the most dangerous neglected tropical diseases, second only to malaria in parasitic causes of death.⁵ Caused by global warming, the endemic regions of leishmaniasis are continuously spreading to nontropical areas, including Europe. So far, no vaccine against leishmaniasis is on the market. Approved drugs in second- and third-line treatments are currently limited and/or exorbitantly priced (i.e., amphotericin B; paromomycin; miltefosine; pentamidine) with a few of them being effective on antimonial-resistant *Leishmania* strains. Moreover, the use of these agents on infected patients is seriously hampered by the insurgence of acute and/or chronic toxicity. Therefore, there is an urgent need for developing safe, effective, and affordable drugs for the treatment of leishmaniasis. To fill this therapeutic gap, several research groups introduced new classes of active compounds against leishmaniasis, including bisindole derivatives.

In this context, phenotypic screening of our small library of previously reported azole-bisindoles **1–3** (Schemes 1 and 2)^{20,25} against four human and canine *L. infantum* strains was performed. With a few exceptions, all bisindoles, belonging to three different classes (pyrroles **1**, imidazoles **2**, and triazoles **3**), showed good activity against the analyzed *L. infantum* promastigotes with IC_{50} values lower than 10 μ M (Table 1).

Conversely, pyrrole-bisindole **1c** is less active than the other compounds, and **1d** and triazole-bisindole **3a** are nearly inactive. At this stage, it seems that an additional nitrogen-containing aryl substituent could increase the potency of the simple bisindole scaffold (**DIM** was almost inactive at 20 μ M). In the pyrrole class **1**, a double substitution of the indole rings is detrimental for their activity (compounds **1c** and **1d** showed low activity). All of the imidazole derivatives **2** are active in all four *L. infantum* promastigote strains, and in particular, **2e** and **2f**, having *N*-methylated indoles, are very potent. The methylation of the indole rings seems to play an important role also in the triazole-bisindole derivatives **3** (**3a** is inactive and **3b** showed $IC_{50} < 8 \mu$ M).

The most active azole-bisindoles **1a**, **URB1483**, **2a–f**, and **3b** were then tested on human and canine macrophage-like cell lines, as well as other human cell lines to check for their potential toxicity. In general, the imidazole-bisindole derivatives **2** are more toxic than pyrroles **1** and triazole **3b** in all of the tested cell lines. Pyrrole-bisindole **URB1483** showed good activity against parasites and the best selectivity index (SI) on both human (THP-1) and canine (DH82) cells (SI > 55, Table 2). Moreover, **URB1483** did not show any appreciable toxicity against human hepatocytes, keratinocytes, and primary fibroblasts (Table S1, Supporting Information).

Although **URB1483** shows high lipophilicity, this feature did not hamper its ability to inhibit leishmanial growth while sparing human cells. For this reason, it was chosen for further studies on other cell models.

Therefore, **URB1483** was tested, in comparison with pentamidine, for its efficacy on *L. infantum*-infected human and canine macrophage-like cell lines. The efficacy of compound **URB1483** and pentamidine was not significantly different in human and canine *in vitro* infection models, despite the fact that pentamidine showed lower IC₅₀ compared to **URB1483** in promastigotes (Table 1). This may account for the better bioavailability of **URB1483** inside the infected cells. Concerning the human infection model (THP-1 cells), the human clinical isolate appeared less susceptible to both drug treatments compared to the reference strain MHOM/TN/80/IPT1. This probably reflects its higher virulence (infection index was twice) and/or its lower susceptibility to treatment with compound **URB1483** (IC₅₀ value was about 2 times higher in the human clinical isolate compared to other strains) (Table 1). As regards the canine infection model, it is noteworthy that pentamidine showed high toxicity in DH82 cells at 72 h (Table 2 and Figure 4), while compound **URB1483** did not show any appreciable toxicity, underlying its potential use also in veterinary applications.

According to the literature, topoisomerase IB was identified as a likely biological target for this class of bisindoles.^{11,12} Furthermore, molecular modeling investigations on topoisomerase IB point to a likely binding mode for **URB1483** similar to the one experimentally observed for topotecan. Therefore, **URB1483** was evaluated for its ability to inhibit on topoisomerase IB from *L. donovani*, which shared 98% sequence identity with *L. infantum* isoform. Unexpectedly, **URB1483** failed to inhibit *L. donovani* topoisomerase IB activity, indicating that other targets are likely engaged by this pyrrole-bisindole. Efforts will be taken to discover the target of **URB1483** in our ongoing research on antileishmanial agents.

CONCLUSIONS

Phenotypic screening of a small library of azole-bisindoles against several human and canine *L. infantum* strains was performed. Most of the tested compounds showed good activity against the promastigotes (IC₅₀ values < 10 μM). **URB1483**, a pyrrole-bisindole derivative, showed good activity against parasites, and it did not affect the viability of canine and human cell lines, with a selectivity index >55. Moreover, the efficacy of **URB1483** on human and canine *in vitro* infection models was comparable to that of the commercial drug pentamidine. Previous works on the bisindole prototype DIM demonstrated that its antileishmanial activity is due to its ability to block the DNA relaxation activity of *Leishmania* topoisomerase IB. This evidence along with computational studies supports the hypothesis that **URB1483** should have worked as a topoisomerase IB inhibitor. Biochemical studies on the isolated enzyme ruled out the inhibition of topoisomerase IB as a mechanism of action for **URB1483**. Even if the search for the biological target is still ongoing, **URB1483** may undoubtedly represent a promising lead compound for the generation of new anti-*Leishmania* agents with low toxicity on host cells.

EXPERIMENTAL SECTION

Materials and Methods. Chemistry. All organic solvents used in this study were purchased from Sigma-Aldrich (St. Louis, MO), Alfa Aesar (Haverhill, MA), or TCI (Tokyo, Japan). In particular, the antileishmanial drugs pentamidine isethionate salt, nonliposomal amphotericin B, and miltefosine, used as positive controls, were purchased from Sigma-Aldrich. Prior to use, acetonitrile, dichloromethane, and toluene were dried with molecular sieves with an effective pore diameter of 4 Å. Column chromatography purifications were performed under “flash” conditions using Merck (Darmstadt, Germany) 230–400 mesh silica gel. Analytical thin-layer chromatography (TLC) was carried out on Merck silica gel plates (silica gel 60 F254), which were visualized by exposure to ultraviolet light and an aqueous solution of cerium ammonium molybdate (CAM). Melting points were determined by Buchi (Gallen, Switzerland) B-540. ¹H NMR and ¹³C NMR spectra were recorded on a Bruker (Billerica, MA) AC 400 and 100 spectrometer, respectively, and analyzed using the TopSpin 1.3 (2013) software package. Chemical shifts were measured using the central peak of the solvent. EI-MS and ESI-MS spectra were recorded with a Shimadzu (Kyoto, Japan) QP-5000 mass spectrometer and with a Waters (Milford, MA) Micromass ZQ spectrometer, respectively. The final compounds were analyzed on a ThermoQuest (Italia) FlashEA 1112 elemental analyzer for C, H, and N. The percentages found were within ±0.5% of the theoretical values. All of the tested compounds were >95% pure as determined by elemental analysis.

General Procedure for the Synthesis of Pyrrole-bisindole Derivatives 1. A mixture of the appropriate bisindole 7¹⁶ (0.4 mmol) and methyl or ethyl propiolate (0.44 mmol) was stirred in DCM (1 mL) overnight at room temperature. A solution of the opportune azoalkene 8 (0.6 mmol) in toluene (4 mL) was added, and the reaction was refluxed for 2 h. A catalytic amount of TFA (two drops) was added, and the reaction was refluxed for an additional 2–4 h (TLC check). After removal of the solvent, the crude mixture was purified by column chromatography on silica gel to afford the corresponding pyrrole-bisindole 1.

The physicochemical data of compounds 1a–d, with purity >95% (determined by elemental analysis), are reported in the Supporting Information, and they are in agreement with those reported in the literature.²⁰

General Procedure for the Synthesis of Imidazole-bisindole Derivatives 2. To a stirred solution of the appropriate bisindole 7¹⁶ (0.4 mmol) in ACN (2 mL), the opportune azoalkene 8 (0.4 mmol) was added at room temperature. After the disappearance of the reagents, checked by TLC analysis (usually 1 h), paraformaldehyde (0.8 mmol) was added, and then the resulting mixture was refluxed for 4 h (TLC check). The solvent was evaporated under reduced pressure, and the crude residue was purified by column chromatography to give the corresponding imidazole-bisindole derivatives 2.

The physicochemical data of compounds 2a–d²⁰ and 2e–f,²⁵ with purity >95% (determined by elemental analysis), are reported in the Supporting Information, and they are in agreement with those reported in the literature.

General Procedure for the Synthesis of Triazole-bisindole Derivatives 3. To a cooled solution (0 °C) of the appropriate bisindole 7¹⁶ (0.4 mmol) in ethanol (5 mL) was added DIPEA (2.4 mmol, 6 equiv). The solution was stirred for 10 min, after

which hydrazine **9** (0.52 mmol, 1.3 equiv) dissolved in acetonitrile (4 mL) was added dropwise to the cooled solution, and stirring was continued at room temperature for 2 h (TLC check). After completion of the reaction, all volatiles were removed under reduced pressure and the residue was purified by column chromatography to give the corresponding triazole-bisindole **3**.

The physicochemical data of compounds **3a,b**, with purity >95% (determined by elemental analysis), are reported in the [Supporting Information](#), and they are in agreement with those reported in the literature.²⁰

Parasite Cultures. The reference strain *L. infantum* MHOM/TN/80/IPT1 (WHO international reference strain) was purchased from ATCC (ATCC 5013). Two *L. infantum* strains were isolated from lymph node aspirates of two infected symptomatic dogs, obtained from the veterinary clinic Santa Teresa (Fano, Italy), as previously described.²¹ Moreover, one *L. infantum* strain was isolated from a skin biopsy taken during a routine diagnostic process from a patient with CL and previously treated with intralesional injections of glucantime.²⁹ All *L. infantum* promastigotes were cultured in Evans' modified Tobie's medium (EMTM) at 26–28 °C. To test bisindole compounds, the parasites were cultivated in RPMI-PY medium as described previously.³⁰

Cell Cultures. The human monocytic cell line THP-1 (ECACC 88081201) was cultured in an RPMI-1640 medium. The canine macrophage-like cell line DH82 (ATCC CRL-10389) and the human hepatocellular carcinoma cell line HepG2 [HEPG2] (ATCC HB-8065) were cultured in Eagle's minimum essential medium (EMEM). Human keratinocyte cell line HaCaT (CLS 300493) and human primary fibroblasts (HPF) from healthy subjects obtained from upper arm skin biopsies, kindly provided by Dr. Giosuè Annibaldi (University of Urbino Carlo Bo), were grown in Dulbecco's modified Eagle's medium (DMEM). All media were supplemented with 10% (15% for DH82 cells) heat-inactivated fetal bovine serum (FBS), 2 mM L-glutamine, 10 g/L nonessential amino acid, 1 mM sodium pyruvate, 100 µg/mL streptomycin, and 100 U/L penicillin. All cell lines were maintained in a humidified incubator at 37 °C and 5% CO₂. All cell culture reagents were purchased from Sigma-Aldrich (St. Louis, MO).

***L. infantum* Promastigotes Viability Assay.** To investigate the bisindole activity on *L. infantum* strains, the late log/stationary phase promastigotes were resuspended in complete RPMI-PY medium at a density of 2.5×10^6 parasites/mL in 96-well plates (100 µL/well). The promastigotes were treated with scalar dilutions 1:2 or 2:3 of the 12 bisindole compounds (from 20 to 0.31 µM) for 72 h at 26 °C. As positive controls, the antileishmanial drugs pentamidine (Sigma-Aldrich) (from 10 to 0.16 µM), nonliposomal amphotericin B (Sigma-Aldrich) (from 1 to 0.0078 µM), and miltefosine (Sigma-Aldrich) (from 20 to 0.31 µM) were included. As the negative control, parasites were treated with the vehicle (DMSO). Each condition was carried out in duplicate. To evaluate the promastigotes viability, the CellTiter 96H Aqueous Non-Radioactive Cell Proliferation Assay (Promega), based on the ability of viable cells to convert a soluble tetrazolium salt [3-(4,5-dimethylthiazol-2-yl)-5-(3-carboxymethoxy-phenyl)-2-(4-sulfophenyl)-2H-tetrazolium. MTS] to a formazan product, was conducted. Briefly, 20 µL of MTS/PMS (phenazine methosulfate, Sigma-Aldrich) was added to 100 µL of culture medium and incubated at 26 °C until formazan production. Absorbance was recorded on a Microplate Reader (Bench-

mark. Bio-Rad) at 492 nm. Results were shown as % of promastigotes growth inhibition compared to control (DMSO). The IC₅₀ values were calculated using nonlinear regression curves in GraphPad Prism 8.0 (GraphPad Software, Inc., San Diego, CA). The equation used for data fitting was $Y = 100 / (1 + 10^{((\text{Log IC}_{50} - X) * \text{Hillslope}))}$ (hillslope not constrained), where X is the log of concentration and Y is the normalized response.

Cytotoxicity Assay. The cytotoxicity of bisindole compounds was evaluated in THP-1, DH82, HEPG2, HaCaT, and HPF cells. THP-1 cells were resuspended at a density of 5×10^6 cells/mL; 100 µL/well were seeded in a 96-well plate and treated with 20 ng/mL phorbol myristic acid (PMA) to induce differentiation into macrophages-like cells for 48 h. DH82 cells were seeded in a 96-well plate with a density of 2×10^5 cells/well and left to attach overnight. After cell adhesion to the plate, selected bisindole compounds were used at concentrations of 2, 10, 20, 80, and 200 µM, for 72 h at 37 °C. Moreover, to test cytotoxicity in actively proliferating cells, DH82, HEPG2, HaCaT, and HPF cells were seeded in a 96-well plate with a density of 2×10^5 cells/well and left to attach overnight; afterward, the cells were treated with selected bisindole compounds at concentrations of 2, 10, and 20 µM, for 24 h at 37 °C. The negative control, (DMSO), and the antileishmanial drugs pentamidine nonliposomal amphotericin B, and miltefosine, were included in each experiment. Each condition was carried out in duplicate. To evaluate the compound cytotoxicity, the CellTiter 96H Aqueous Non-Radioactive Cell Proliferation Assay (Promega) was conducted as described above. For each compound, the selectivity index (SI) was calculated as the ratio between cytotoxicity in THP-1 and DH82 cells (CC₅₀, 72 h) and activity against *L. infantum* promastigotes (IC₅₀, 72 h).

Antiamastigote Assay on Infected Cells. The activity of **URB1483** against intracellular amastigotes was evaluated in THP-1- and DH82-infected cells. Briefly, THP-1 cells were seeded in 35 mm dishes with a density of 6×10^5 cells/dish and treated with 20 ng/mL phorbol myristic acid (PMA) for 48 h to induce differentiation into macrophage-like cells. After differentiation, the cells were infected for 24 h with *L. infantum* MHOM/TN/80/IPT1 (or human clinical isolate) promastigotes with a parasite-to-cell ratio of 10:1. Noninternalized promastigotes were then removed and the cells were treated with **URB1483** or with the positive control pentamidine at concentrations of 2, 10, and 20 µM, for 72 h. DH82 cells were seeded at a density of 2.5×10^5 cells/dish in 35 mm dishes for 24 h. The infection and treatment were performed as described above. Since the vehicle DMSO did not show any toxicity on *L. infantum* promastigotes or on mammalian cells, it was not included in the experiments of infection.

To monitor the infection, the cells were washed, formaldehyde/methanol fixed, stained with Hoechst dye, and observed with a fluorescence microscope. The infection index (percentage of infected macrophages × the average number of parasites per macrophage) was obtained by counting at least 300 cells for each condition.

Statistical Analysis. The evaluation of IC₅₀ in promastigotes and CC₅₀ in mammalian cells following bisindole treatment was performed by nonlinear regression analysis and expressed as mean and 95% confidence interval. Statistical analyses of infection indexes were performed using one-way ANOVA followed by Tukey's multiple-comparison post hoc test and two-way ANOVA followed by Bonferroni correction for

multiple comparisons. All tests were performed using GraphPad Prism version 8 (GraphPad Software, Inc., La Jolla, CA). A p value ≤ 0.05 was considered significant.

Molecular Modeling. Model Building. Differently from human topoisomerase I (hTopo I), which is produced as a monomeric enzyme composed of a single 765 residue polypeptide chain, *L. donovani* topoisomerase I is a heterodimeric protein composed of a large subunit (LdTOP1L) of 635 residues and a small subunit (LdTOP1S) of 262 residues. Despite this different organization, superposition of LdTOP1LS heterodimer (PDB ID 2B9S)²⁷ bound to DNA on the structure of hTopo I bound to DNA complexed with topotecan (PDB ID 1K4T)²⁶ reveals that the amino acids shaping the drug-binding cavity are conserved between the two species. Moreover, both human and *L. donovani* forms undertook similar interactions with the 22-bp DNA duplex oligonucleotide present in both the X-ray structures. The key difference between the two PDB complexes resides in the size of the major groove of the DNA double strand, which is slightly larger in human form, where the topotecan is accommodated. Using available structural information here summarized, a 3D model of *L. donovani* topoisomerase I bound to DNA-topotecan complex was built using Maestro 11.6³¹ within the Schrodinger 2018–2 software, following the computational protocol reported by Roy et al.¹² In brief, after superposing the backbone atoms of the LdTOP1LS heterodimer on the backbone atoms hTopo I protein, the DNA double strand of *Leishmania donovani* isoform was replaced with the DNA double strand present in the hTopo I-DNA-topotecan complex. The resulting LdTOP1LS-DNA-topotecan ternary complex was submitted to a protocol of geometry optimization based on energy minimization using OPLS3e force field.³² After deletion of topotecan from the binding site, the resulting structure was employed to perform docking simulation with Glide 7.9 software.³³

Ligand Docking. Docking studies were performed with Glide included in the Schrodinger software package³⁴ starting from LdTOP1LS-DNA-topotecan ternary model described above, following a protocol successfully applied to predict the docking pose of indole-containing compounds.³⁵ The docking grid was centered on the position of topotecan ligand. Dimensions of enclosing and bounding boxes were set to 20 and 10 Å on each side, respectively, and van der Waals radii of protein atoms were not scaled during grid generation. The structure of URB1483 was built in Maestro and then energy-minimized in implicit solvent (water) with OPLS3e force field to an energy gradient of 0.01 kcal/(mol Å). The minimized ligands were docked within the topotecan-binding site (see above) using Glide software in Standard Precision mode with default settings. Poses were ranked according to the Gscore value.

Stability Studies of URB1483. An opportune aliquot of a stock solution of URB1483 in DMSO (10 mM) were added to a physiological solution (0.90% w/v of NaCl water solution) or EMEM or EMTM (URB1483 concentration = 50 μ M) and maintained at 37 °C. At regular time points, aliquots of the described solutions were sampled, two volumes of ACN were added, and samples were centrifuged (8000 rpm, 10 min) and analyzed by HPLC-ESI-MS for a percentage of the remaining compound over incubation time.

■ ASSOCIATED CONTENT

Supporting Information

The Supporting Information is available free of charge at <https://pubs.acs.org/doi/10.1021/acsomega.1c05611>.

Physicochemical data of azole-bisindoles 1–3; graphical representations of MTS assays with various concentrations of azole-bisindoles and three commercial drugs used as positive controls on four *L. infantum* promastigote strains (IC₅₀ reported in Table 1, main text); graphical representations of MTS assays with various concentrations of selected azole-bisindoles and three commercial drugs on human (THP-1) and canine (DH82) macrophages for 72 h treatments (CC₅₀ reported in Table 2, main text); cytotoxicity of selected azole-bisindoles after 24 h treatment in canine DH82 macrophages and three different human cell lines (HEPG2, HaCaT, and HPF); two-way ANOVA results of treatment with compound URB1483 and pentamidine in three different infection models; superposition of the docking pose of URB1483 within the *L. donovani* topoisomerase IB on the indolocarbazole inhibitor SA315F reported in the ternary adduct involving DNA and human topoisomerase IB; inhibition studies of the *L. donovani* and human topoisomerase IB activities by URB1483; predicted log p values of azole-bisindoles and reference compounds; LC/MS (SIR) chromatograms of the experiment regarding the stability of URB1483; and references (PDF)

■ AUTHOR INFORMATION

Corresponding Author

Simone Lucarini – Department of Biomolecular Sciences, University of Urbino Carlo Bo, 61029 Urbino (PU), Italy; orcid.org/0000-0002-3667-1207; Phone: +39 0722 303333; Email: simone.lucarini@uniurb.it

Authors

Aurora Diotallevi – Department of Biomolecular Sciences, University of Urbino Carlo Bo, 61029 Urbino (PU), Italy; orcid.org/0000-0001-5456-1821

Laura Scalvini – Department of Food and Drug, University of Parma, 43124 Parma, Italy; orcid.org/0000-0003-3610-527X

Gloria Buffi – Department of Biomolecular Sciences, University of Urbino Carlo Bo, 61029 Urbino (PU), Italy; orcid.org/0000-0001-6288-8787

Yolanda Pérez-Pertejo – Department of Biomedical Sciences, University of León, 24071 León, Spain

Mauro De Santi – Department of Biomolecular Sciences, University of Urbino Carlo Bo, 61029 Urbino (PU), Italy

Michele Verboni – Department of Biomolecular Sciences, University of Urbino Carlo Bo, 61029 Urbino (PU), Italy; orcid.org/0000-0001-5648-521X

Gianfranco Favi – Department of Biomolecular Sciences, University of Urbino Carlo Bo, 61029 Urbino (PU), Italy; orcid.org/0000-0003-3112-819X

Mauro Magnani – Department of Biomolecular Sciences, University of Urbino Carlo Bo, 61029 Urbino (PU), Italy
Alessio Lodola – Department of Food and Drug, University of Parma, 43124 Parma, Italy; orcid.org/0000-0002-8675-1002

Luca Galluzzi – Department of Biomolecular Sciences,
University of Urbino Carlo Bo, 61029 Urbino (PU), Italy;
orcid.org/0000-0002-1747-526X

Complete contact information is available at:
<https://pubs.acs.org/10.1021/acsomega.1c05611>

Author Contributions

M.V., G.F., and S.L. synthesized the azole-bisindole derivatives and studied the stability properties of URB1483. A.D., G.B., M.D.S., and L.G. designed and performed biological assays on *L. infantum* protozoa, canine, and human cell lines. L.S. and A.L. designed and performed docking studies. Y.P.-P. designed and performed DNA relaxation assay and agarose cleaving assay on human and *L. donovani* topoisomerase IB. M.M. and S.L. performed funding acquisition. A.L., S.L., and L.G. analyzed data and wrote the original manuscript. All of the authors reviewed and edited the manuscript and approved the final version.

Notes

The authors declare no competing financial interest.

ACKNOWLEDGMENTS

The authors thank Prof. Alessandro Desideri, Dr. Silvia Castelli (University of Rome “Tor Vergata”), and Prof. Rafael Balaña-Fouce (University of Leon, Spain) for the inhibition studies on Human and *Leishmania* Topoisomerase IB and fruitful discussions. They are also grateful to Dr. Giosuè Annibalini (University of Urbino Carlo Bo) for providing HPF cells and Dr. Lucia Vedovi (University of Urbino Carlo Bo) for the extensive editing of the English language and style of the manuscript. This work was partially supported by University of Urbino Carlo Bo, FANOATENEIO and FFABR (fund for basic research activities) from MIUR (Italian Ministry of Education, University and Research).

ABBREVIATIONS USED

CL, Cutaneous Leishmaniasis; ML, Mucosal Leishmaniasis; VL, visceral leishmaniasis; *L.*, *Leishmania*; DIM, 3,3'-diindolylmethane; DIMs, 3,3'-diindolylmethane derivatives; CPT, camptothecin; DPDIM, 2,2'-diphenyl-3,3'-diindolylmethane; ACN, acetonitrile; DIPEA, *N,N*-diisopropylethylamine; Pent, pentamidine; Amph B, nonliposomal amphotericin B; Milt, miltefosine; HPF, human primary fibroblasts; hTopo I, human topoisomerase IB; LdTOP1L, *L. donovani* topoisomerase IB large subunit; LdTOP1S, *L. donovani* topoisomerase IB small subunit; EMEM, Eagle's minimum essential medium; DMEM, Dulbecco's modified Eagle's medium; FBS, fetal bovine serum; RMSD, root-mean-square deviation

REFERENCES

- (1) Nagle, A. S.; Khare, S.; Kumar, A. B.; Buchynskyy, F. S. A.; Mathison, C. J. N.; Chennamaneni, N. K.; Pendem, N.; Buckner, F. S.; Gelb, M. H.; Molteni, V. Recent developments in drug discovery for leishmaniasis and human african trypanosomiasis. *Chem. Rev.* **2014**, *114*, 11305–11347.
- (2) Ortalli, M.; Mistral De Pascali, A.; Longo, S.; Pascarelli, N.; Porcellini, A.; Ruggeri, D.; Randi, V.; Procopio, A.; Re, M. C.; Varani, S. Asymptomatic *Leishmania infantum* infection in blood donors living in an endemic area, northeastern Italy. *J. Infect.* **2020**, *80*, 116–120.
- (3) Catta-Preta, C. M. C.; Mottram, J. C. Drug candidate and target for leishmaniasis. *Nature* **2018**, *560*, 171–172.
- (4) Di Muccio, T.; Scalone, A.; Bruno, A.; Marangi, M.; Grande, R.; Armignacco, O.; Gradoni, L.; Gramiccia, M. Epidemiology of

imported leishmaniasis in Italy: implications for a European endemic country. *PLoS One* **2015**, *10*, No. e0129418.

(5) Srivastava, S.; Shankar, P.; Mishra, J.; Singh, S. Possibilities and challenges for developing a successful vaccine for leishmaniasis. *Parasites Vectors* **2016**, *9*, No. 277.

(6) Ponte-Sucre, A.; Gamarro, F.; Dujardin, J.-C.; Barrett, M. P.; López-Vélez, R.; García-Hernández, R.; Pountain, A. W.; Mwenechanya, R.; Papadopolou, B. Drug resistance and treatment failure in leishmaniasis: A 21st century challenge. *PLoS Negl. Trop. Dis.* **2017**, *11*, No. e0006052.

(7) Bekhit, A. A.; El-Agroudy, E.; Helmy, A.; Ibrahim, T. M.; Shavandi, A.; Bekhit, A. E.-D. A. *Leishmania* treatment and prevention: natural and synthesized drugs. *Eur. J. Med. Chem.* **2018**, *160*, 229–244.

(8) Sangshetti, J. N.; Kalam Khan, F. A.; Kulkarni, A. A.; Aroteb, R.; Patil, R. H. Antileishmanial drug discovery: comprehensive review of the last 10 years. *RSC Adv.* **2015**, *5*, 32376–32415.

(9) Razzaghi-Asl, N.; Sepehri, S.; Ebadi, A.; Karami, P.; Nejatkhah, N.; Johari-Ahar, M. Insights into the current status of privileged *N*-heterocycles as antileishmanial agents. *Mol. Diversity* **2020**, *24*, 525–569.

(10) Cavalli, A.; Bolognesi, M. L. Neglected tropical diseases: multi-target-directed ligands in the search for novel lead candidates against *Trypanosoma* and *Leishmania*. *J. Med. Chem.* **2009**, *52*, 7339–7359.

(11) Roy, A.; Das, B. B.; Ganguly, A.; Dasgupt, S. B.; Khalkho, N. V. M.; Pal, C.; Dey, S.; Giri, V. S.; Jaisankar, P.; Dey, S.; Majumder, H. K. An insight into the mechanism of inhibition of unusual bi-subunit topoisomerase I from *Leishmania donovani* by 3,3'-di-indolylmethane, a novel DNA topoisomerase I poison with a strong binding affinity to the enzyme. *Biochem. J.* **2008**, *409*, 611–622.

(12) Roy, A.; Chowdhury, S.; Sengupta, S.; Mandal, M.; Jaisankar, P.; D'Annessa, I.; Desideri, A.; Majumder, H. K. Development of derivatives of 3,3'-diindolylmethane as potent *Leishmania donovani* bi-subunit Topoisomerase IB poisons. *PLoS One* **2011**, *6*, No. e28493.

(13) Bharate, S. B.; Bharate, J. B.; Khan, S. I.; Tekwani, B. L.; Jacob, M. R.; Mudududdla, R.; Yadav, R. R.; Singh, B.; Sharma, P. R.; Maity, S.; Singh, B.; Khan, I. A.; Vishwakarma, R. A. Discovery of 3,3'-diindolylmethanes as potent antileishmanial agents. *Eur. J. Med. Chem.* **2013**, *63*, 435–443.

(14) Kalam Khan, F. A.; Zaheer, Z.; Sangshetti, J. N.; Patil, R. H.; Farooqui, M. Antileishmanial evaluation of clubbed bis(indolyl)-pyridine derivatives: one-pot synthesis, *in vitro* biological evaluations and *in silico* ADME prediction. *Bioorg. Med. Chem. Lett.* **2017**, *27*, 567–573.

(15) Taha, M.; Uddin, I.; Gollapalli, M.; Almandil, N. B.; Rahim, F.; Farooq, R. K.; Nawaz, M.; Ibrahim, M.; Alqahtani, M. A.; Bamarouf, Y. A.; Selvaraj, M. Synthesis, anti-leishmanial and molecular docking study of bis-indole derivatives. *BMC Chem.* **2019**, *13*, No. 102.

(16) Mari, M.; Tassoni, A.; Lucarini, S.; Fanelli, M.; Piersanti, G.; Spadoni, G. Brønsted acid catalyzed bisindolization of α -amido acetals: synthesis and anticancer activity of bis(indolyl)ethanamine derivatives. *Eur. J. Org. Chem.* **2014**, *2014*, 3822–3830.

(17) Salucci, S.; Burattini, S.; Buontempo, F.; Orsini, E.; Furiassi, L.; Mari, M.; Lucarini, S.; Martelli, A. M.; Falcieri, E. Marine bisindole alkaloid: a potential apoptotic inducer in human cancer cells. *Eur. J. Histochem.* **2018**, *62*, No. 2881.

(18) Campana, R.; Favi, G.; Baffone, W.; Lucarini, S. Marine alkaloid 2, 2-bis(6-bromo-3-indolyl) ethylamine and its synthetic derivatives inhibit microbial biofilms formation and disaggregate developed biofilms. *Microorganisms* **2019**, *7*, 28.

(19) Campana, R.; Sisti, M.; Sabatini, L.; Lucarini, S. Marine bisindole alkaloid 2,2-bis(6-bromo-3-indolyl) ethylamine to control and prevent fungal growth on building material: a potential antifungal agent. *Appl. Microbiol. Biotechnol.* **2019**, *103*, 5607–5616.

(20) Mantenuto, S.; Lucarini, S.; De Santi, M.; Piersanti, G.; Brandi, G.; Favi, G. One-pot synthesis of biheterocycles based on indole and azole scaffolds using tryptamines and 1,2-diaza-1,3-dienes as building blocks. *Eur. J. Org. Chem.* **2016**, *19*, 3193–3199.

(21) Galluzzi, L.; Diotallevi, A.; De Santi, M.; Ceccarelli, M.; Vitale, F.; Brandi, G.; Magnani, M. *Leishmania infantum* induces mild unfolded protein response in infected macrophages. *PLoS One* **2016**, *11*, No. e0168339.

(22) Diotallevi, A.; De Santi, M.; Buffi, G.; Ceccarelli, M.; Vitale, F.; Galluzzi, L.; Magnani, M. *Leishmania* infection induces MicroRNA hsa-mir-346 in human cell line-derived macrophages. *Front. Microbiol.* **2018**, *9*, No. 1019.

(23) Diotallevi, A.; Buffi, G.; Ceccarelli, M.; Neitzke-Abreu, H. C.; Gnutzmann, L. V.; da Costa Lima, M. S.; Di Domenico, A.; De Santi, M.; Magnani, M.; Galluzzi, L. Real-time PCR to differentiate among *Leishmania* (*Viamnia*) subgenus, *Leishmania* (*Leishmania*) *infantum* and *Leishmania* (*Leishmania*) *amazonensis*: application on Brazilian clinical samples. *Acta Trop.* **2020**, *201*, No. 105178.

(24) Ceccarelli, M.; Diotallevi, A.; Andreoni, F.; Vitale, F.; Galluzzi, L.; Magnani, M. Exploiting genetic polymorphisms in metabolic enzymes for rapid screening of *Leishmania infantum* genotypes. *Parasites Vectors* **2018**, *11*, No. 572.

(25) Mantenuto, S.; Ciccolini, C.; Lucarini, S.; Piersanti, G.; Favi, G.; Mantellini, F. Palladium(II)-catalyzed intramolecular oxidative C–H/C–H cross-coupling reaction of C3,N-linked biheterocycles: rapid access to polycyclic nitrogen heterocycles. *Org. Lett.* **2016**, *19*, 608–611.

(26) Staker, B. L.; Hjerrild, K.; Feese, M. D.; Behnke, C. A.; Burgin, A. B.; Stewart, L. The mechanism of topoisomerase I poisoning by a camptothecin analog. *Proc. Natl. Acad. Sci. USA* **2002**, *99*, 15387–15392.

(27) Davies, D. R.; Mushtaq, A.; Interthal, H.; Champoux, J. J.; Hol, W. G. The structure of the transition state of the heterodimeric topoisomerase I of *Leishmania donovani* as a vanadate complex with nicked DNA. *J. Mol. Biol.* **2006**, *357*, 1202–1210.

(28) Staker, B. L.; Feese, M. D.; Cushman, M.; Pommier, Y.; Zembower, D.; Stewart, L.; Burgin, A. B. Structures of three classes of anticancer agents bound to the human topoisomerase I-DNA covalent complex. *J. Med. Chem.* **2005**, *48*, 2336–2345.

(29) Diotallevi, A.; Buffi, G.; Corbelli, G.; Ceccarelli, M.; Ortalli, M.; Varani, M.; Magnani, M.; Galluzzi, L. In vitro reduced susceptibility to pentavalent antimonials of a *Leishmania infantum* isolate from a human cutaneous leishmaniasis case in central Italy. *Microorganisms* **2021**, *9*, No. 1147.

(30) Castelli, G.; Galante, A.; Lo Verde, V.; Migliazzo, A.; Reale, S.; Lupo, T.; Piazza, M.; Vitale, F.; Bruno, F. Evaluation of two modified culture media for *Leishmania infantum* cultivation versus different culture media. *J. Parasitol.* **2014**, *100*, 228–230.

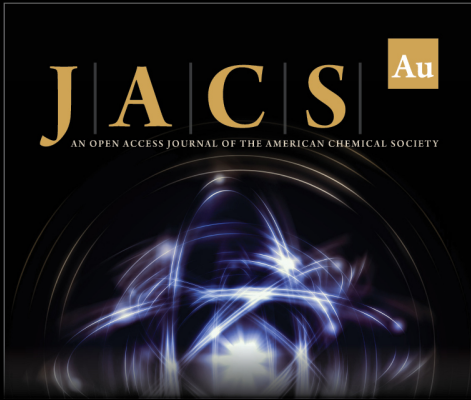
(31) *Schrödinger Release 2018-2: Maestro*, Schrödinger, LLC: New York, NY, 2018.

(32) Roos, K.; Wu, C.; Damm, W.; Reboul, M.; Stevenson, J. M.; Lu, C.; Dahlgren, M. K.; Mondal, S.; Chen, W.; Wang, L.; Abel, R.; Friesner, R. A.; Harder, E. D. OPLS3e: Extending Force Field Coverage for Drug-Like Small Molecules. *J. Chem. Theory Comput.* **2019**, *15*, 1863–1874.

(33) Friesner, R. A.; Banks, J. L.; Murphy, R. B.; Halgren, T. A.; Klicic, J. J.; Mainz, D. T.; Repasky, M. P.; Knoll, E. H.; Shelley, M.; Perry, J. K.; Shaw, D. E.; Francis, P.; Shenkin, P. S. Glide: a new approach for rapid, accurate docking and scoring. 1. Method and assessment of docking accuracy. *J. Med. Chem.* **2004**, *47*, 1739–1749.


(34) Schrödinger, LLC, 2019. New York, NY.


(35) Spadoni, G.; Bedini, A.; Furiassi, L.; Mari, M.; Mor, M.; Scalvini, L.; Lodola, A.; Ghidini, A.; Lucini, V.; Dugnani, S.; Scaglione, F.; Piomelli, D.; Jung, K.-M.; Supuran, C. T.; Lucarini, L.; Durante, M.; Sgambellone, S.; Masini, E.; Rivara, S. Identification of bivalent ligands with melatonin receptor agonist and fatty acid amide hydrolase (FAAH) inhibitory activity that exhibit ocular hypotensive effect in the rabbit. *J. Med. Chem.* **2018**, *61*, 7902–7916.



JACS Au
AN OPEN ACCESS JOURNAL OF THE AMERICAN CHEMICAL SOCIETY

Editor-in-Chief
Prof. Christopher W. Jones
Georgia Institute of Technology, USA

Open for Submissions 

pubs.acs.org/jacsau  ACS Publications
Most Trusted. Most Cited. Most Read.